The DOI for this manuscript is doi: 10.1175/JAS-D-13-0190.1

Parameter study of tropical cyclones in rotating radiative-convective equilibrium with column physics and resolution of a 25 km GCM

Wenyu Zhou

Atmospheric and Oceanic Sciences Program, Princeton University, Princeton, New Jersey

Isaac M. Held

Geophysical Fluid Dynamics Laboratory/NOAA, Princeton, New Jersey

Stephen T. Garner

Geophysical Fluid Dynamics Laboratory/NOAA, Princeton, New Jersey

ABSTRACT

Rotating radiative-convective equilibrium is studied by extracting the column physics of a meso-scale resolution global atmospheric model that simulates realistic hurricane frequency statistics and coupling it to rotating hydrostatic dynamics in doubly-periodic domains. The parameter study helps in understanding the tropical cyclones simulated in the global model and also provides a reference point for analogous studies with cloud resolving models.

The authors first examine the sensitivity of the equilibrium achieved in a large square domain (2×10^4 km on a side) to sea surface temperature, ambient rotation rate and surface drag coefficient. In such a large domain, multiple tropical cyclones exist simultaneously. The size and intensity of these tropical cyclones are investigated.

The variation of rotating radiative-convective equilibrium with domain size is also studied. As domain size increases, the equilibrium evolves through four regimes: a single tropical depression, an intermittent tropical cyclone with intensity widely varying, a single sustained storm, and finally multiple storms. As SST increases or ambient rotation rate f decreases, the sustained storm regime shifts towards larger domain size. The storm's natural extent in large domains can be understood from this regime behavior.

The radius of maximum surface wind, although only marginally resolved, increases with SST and increases with f for small f when the domain is large enough. But these parameter dependencies can be modified or even reversed if the domain is smaller than the storm's natural extent.

1. Introduction

Rotating radiative-convective equilibrium, achieved in a doubly periodic box on an f-plane with horizontally homogeneous forcing and boundary condition, is an informative idealized framework for studying the interactions between moist thermodynamics, radiation, and rotating dynamics. It can be studied in non-hydrostatic models in which deep convection is partly resolved and also in lower resolution hydrostatic models with parameterized convection. In the latter case, one can think of this framework as one of a hierarchy of idealized settings in which to study the implications of the assumptions made in GCMs.

Tropical cyclones (TCs) form within these rotating radiative-convective equilibria, and they provide simulations in which very long-lived mature TCs emerge. If run at the resolution and with the column physics (including boundary layer, radiation, microphysics, moist convection and cloud modules) of a global comprehensive model, this idealized framework can help us evaluate the TC simulations in such models. Global models are moving to high enough resolution that aspects of their TC simulations are becoming more realistic, and these global models are one of the tools being used to try to predict the impact of climate change on TC statistics. Being able to study the model-generated TCs in this idealized geometry, eventually comparing to analogous simulations at cloud-resolving resolutions, should provide valuable information as to the limitations and strengths of the TC simulations in global models.

Held and Zhao (2008, hereafter HZ08) describe such a rotating radiative-convective equilibrium in which the column physics of a particular atmospheric model, GFDL's AM2 (Atmospheric Model version 2) is coupled to rotating hydrostatic dynamics in a doubly-periodic box. A similar equilibrium is achieved in Nolan et al. (2007) and Nolan and Rappin (2008) with higher cloud-resolving resolution in a study of tropical cyclogenesis. Schecter and Dunkerton (2009) and Schecter (2011) set up an idealized three-layer hurricane model under such a framework, with simplified radiative and convective parameterizations. The variability and predictability of hurricanes in rotating radiative-convective equilibrium is studied by

Hakim (2011), Hakim (2013), and Brown and Hakim (2013) using both axisymmetric and three-dimensional models.

Besides their various choices for column physics and resolution, a major difference among these studies is that HZ08 considers a sufficiently large domain for multiple TCs to coexist while others use small domains within which only one TC develops. In those small-domain simulations, whether with a doubly-periodic domain or a rigid-wall box, the extent of TCs is explicitly set by the domain size. Because of this constraint, both the state of equilibrium achieved and its parameter sensitivity may be interfered with by the domain size. We refer to our doubly-periodic small-domain simulation as *lattice* equilibrium, in which duplicated TCs exist simultaneously at the grid points in a lattice that can be visualized by duplicating the doubly-periodic domain along its boundaries. The large-domain simulations avoid such finite-domain effects and can be regarded as *turbulent* equilibria in the sense that multiple TCs interact with respect to each other in more complex ways. The extent of TCs is thus controlled by internal processes of the turbulent equilibrium instead of domain size. This allows for analysis of size and intensity of TCs as a function of environmental parameters, independent of domain size. Neither configuration is realistic in the sense that appropriate decay mechanisms (poleward drift and interactions with land and extratropical systems) and suppression factors (wind shear, subsidence and dry air entrainment) are not present, resulting in very long-lived storms.

In this study, both lattice and turbulent equilibria are achieved in doubly-periodic domains, with column physics and resolution of a 25 km global atmospheric model, which simulates many aspects of tropical cyclone statistics realistically (Zhao et al. 2009). The details of model formulation are presented in section 2. We start by describing turbulent equilibrium achieved in a large domain (2×10^4 km on a side) in section 3. The parameter sensitivity of TC structure and intensity in this turbulent equilibrium is studied by varying sea surface temperature, ambient rotation rate f and surface drag coefficient C_D. In section 4, we explore the variation of lattice equilibrium as a function of domain size, and show how the natural extent of TCs in turbulent equilibrium is related to this domain size dependency of lattice equilibrium. A discussion and conclusion are offered in section 5.

One of our goals is to map out some of these parameter dependencies in the hope of encouraging the study of other GCM's column physics in this idealized setting. We believe that understanding these parameter dependencies and how they differ between parameterized-convection hydrostatic and cloud-resolving non-hydrostatic models will be helpful in evaluating the simulations of TC statistics in global models in the future. To the extent that reliable cloud-resolving simulations are available, this idealized rotating radiative-convective equilibrium framework could also be used as a novel test for the performance of convection schemes.

2. Model formulation

The column physics used here is that of HiRAM (GFDL High Resolution Atmospheric Model). HiRAM has been used in Zhao et al. (2009) to realistically simulate the observed global climatology and interannual variability of hurricane frequency at 50 km resolution, although few storms are simulated higher than category 2 as measured by the maximum surface winds, especially in the N.Atlantic (Zhao and Held 2010). Multiple simulations of the period 1979-2008, running over observed sea surface temperatures, with both 50 km and 25 km resolution versions of this model have been placed in the CMIP5 (Climate Model Intercomparison Project Version 5) archive. The seasonal and interannual variability of tropical storm genesis is not fundamentally different in the 25 and 50 km models. A 25 km version of the model with modified surface flux formulation and microphysical scheme has shown impressive skill for seasonal forecasts in the Atlantic (Chen and Lin 2012).

HiRAM was developed starting from an earlier lower resolution model, AM2 (GAMDT 2004). The prognostic cloud fraction scheme is changed to a simpler diagnostic scheme assuming a sub-grid scale distribution of total water. The relaxed Arakawa-Schubert convective closure (Moorthi and Suarez 1992) in AM2 has been replaced by a modified shallow convection scheme (Bretherton et al. 2004 and Zhao et al. 2009), which results in a larger fraction of precipitation occurring at resolved scale rather than through the parameterization. All other physical schemes are the same as in AM2. Surface fluxes are computed using Monin-Obukhov similarity theory, with a gustiness component (1 m s^{-1}) to account for contribution from sub-grid wind fluctuation (Beljaars 1995). Oceanic roughness lengths are prescribed according to Beljaars (1995). For vertical diffusion, a K-profile scheme designed for cloud-topped boundary layers, with parameterized entrainment rates at the top of the boundary layer (Lock et al. 2000) is used. Stability functions with thresholds dependent on Richardson number are adopted for stable layers. We refer the reader to GAMDT (2004) and Zhao et al. (2009) for further details.

The doubly-periodic model has the same vertical level altitudes as the GCM with the lowest level at about 35 m. The horizontal resolution is 25 km. As in HZ08, there is no diurnal or seasonal cycle in the doubly periodic model, and the radiative forcing is configured using an equatorial annual mean solar zenith angle. Sea surface temperatures are homogeneously prescribed over a saturated (ocean) surface. Aerosols are absent in the atmosphere, while the stratospheric ozone is fixed at an observed tropically-averaged vertical profile.

The homogeneous doubly-periodic f-plane framework contains none of the synoptic variability that helps control TC genesis in the HiRAM global models, but the genesis frequency in those models is not simply a product of downscale transfer from larger scales; it is also a function of parameters in the convection scheme (Zhao et al. 2012). As one example, if one suppresses deep convection very strongly by increasing the strength of entrainment into the parameterizations deep convective cores, the number of TCs that form in the global model is reduced dramatically. Very similar behavior is found in our homogeneous f-plane simulations. We hope to describe the dependence of rotating radiative-convective equilibria at this resolution on the convection scheme elsewhere.

3. Varying environmental parameters in turbulent equilibrium

Turbulent equilibrium is achieved using a large domain (2×10^4 km)^2. The initial condition is an observed tropically-averaged temperature profile, with moisture artificially near saturation below 100 hPa. The model is integrated 2.5 years to its equilibrium. Most statistics, such as hydrological balance, do not require this long an integration. After the initial genesis period a qualitative equilibrium is typically achieved in a few months, but the number of TCs usually decreases slowly with time until it is finally stable. While we cannot prove that the TC number would not decrease with even longer integrations, the behavior seen in the last 6 months of the simulations is a statistically stationary number of cyclones, with the occasional collapse or merger event followed by genesis into the space left by this event. For every 3-hourly output during the last 6 months of each simulation, TCs are collected by identifying points with surface pressure p_s satisfying two criteria: 1) p_s is less than a critical value of 990 hPa, and 2) p_s is a minimum at this point within the surrounding 10×10 grid box.

We first look at the sensitivity to SST, with ambient rotation rate set at 20°N. Snapshots of surface wind speed for two different SSTs are compared in Fig. 1. As found in HZ08, the number of TCs decreases with SST. There are about 40 TCs within the domain for SST at 297 K but only about 15 TCs for SST at 305 K. The distribution of TC central surface pressure is shown in Fig. 2a. The peak frequency of TC central surface pressure shifts towards a lower value as SST increases, indicating consistent higher intensity at warmer SST. The mean central surface pressure intensifies by about 3 hPa K^{-1} and the mean maximum surface wind speed (the wind in the lowest model layer, at roughly 35 m) increases roughly 1.5 m s^{-1} K^{-1} (Fig. 3a and 3b). This is comparable to the sensitivity found in the global model, which indicates roughly a 4 m s^{-1} increase in the mean maximum surface wind between the case with climatological SST and that with 2 K increases in SST (Zhao and Held 2010).

Potential intensity (PI) is computed from the time- and domain-mean thermodynamic profiles, following Bister and Emanuel (2002a) [1]. We choose the option of pseudo-adiabatic ascent and include dissipative heating (as in the GCM, the kinetic energy dissipation in the boundary layer is returned as heat within the boundary layer). The ratio of surface exchange coefficient for enthalpy C_k to surface drag coefficient C_D is set at 0.6, to be consistent with the ratios produced in the model. A velocity reduction factor of 0.9 is applied as a way to extrapolate down through the frictional boundary layer (Bister and Emanuel 2002b). The theoretical maximum wind speed captures the slope of intensification with SST quite well except for very low SSTs (Fig. 3). The explanation for this mismatch at lower SSTs may be that over such cold SST TCs are too weak to compete with random convection and have difficulty in maintaining their mature state. Note that although the theoretical maximum wind speed always exceeds the simulated wind speed, the theoretical pressure perturbation is generally weaker than that in the simulation. Whatever the reason for this difference, the behavior of TCs in the GCM is similar: minimum central surface pressures are comparable to the PI's theory but TCs never reach beyond category 2 in term of maximum wind (Zhao and Held 2010).

The sensitivity to ambient rotation rate f is investigated by varying f from 5°N to 20°N with fixed SST at 301 K. Snapshots of surface wind for f at 5°N and 20°N are compared in Fig. 4. As found in HZ08, the number of TCs increases with ambient rotation rate. There are about 23 TCs within the domain for f at 20°N but only about 5 TCs for f at 5°N. The peak frequency of TC central surface pressure shifts towards higher value as f increases, indicating weaker intensity at larger f (Fig. 2b). As f increases from 5°N to 20°N, the mean central surface pressure (Fig. 3c) increases by 30$\sim$40 hPa, and by the same measures the mean maximum surface wind (Fig. 3d) decreases by 5$\sim$10 m s^{-1}. The difference in vertical profiles of temperature and specific humidity show a moister and warmer environment for larger ambient rotation rate (Fig. 5). The increasing air temperature and

[1] utilizing the code provided at ftp://texmex.mit.edu/pub/emanuel/TCMAX/

humidity at the surface corresponds to a reduced surface moisture disequilibrium. The domain-averaged evaporation and precipitation do not change substantially, as expected from the close balance between radiation cooling and latent heat flux, but the average surface wind speed increases due to the increased density of TCs. We interpret the reduction in surface disequilibrium as determined by the need to maintain the same strength of hydrological cycle in the presence of stronger mean surface wind. The increasing of temperature is amplified upward, approximately following a moist adiabat. The pattern of temperature and humidity differences also indicates more aggressive shallow convection in the cases with larger ambient rotation rate. The potential intensity computed from this vertical profile satisfactorily captures the decreasing intensity with increasing f.

To study the sensitivity to surface drag coefficient, we bypass the Monin-Obukhov scheme and prescribe surface exchange coefficients homogeneously within the domain. The surface drag coefficient C_D is varied from 0.6×10^{-3} to 2.4×10^{-3}, while the surface exchange coefficient for enthalpy C_k is fixed at 1.2×10^{-3}. Three sets of experiments are conducted with ambient rotation rate set at 10°N, 15°N and 20°N. The distribution of TC central surface pressure is shown in Fig. 6. Interestingly, this curve shifts with C_D in opposite direction for different rotation rates. For smaller C_D, there are more intense TCs with f set at 10°N but more weak TCs with f set at 20°N. In spite of this difference, the number of TCs within the domain decreases with C_D in all three cases (as can be seen in Fig. 6).

The sensitivity of TC intensity to C_D is summarized in Fig. 3e and 3f, with ambient rotation rate chosen at 15°N. As C_D decreases from 2.4×10^{-3} to 0.6×10^{-3}, the mean central surface pressure intensifies by only about 10 hPa and the mean maximum surface wind increases by roughly 50%. The difference in vertical profiles of temperature and specific humidity are shown in Fig 5, indicating a warmer and more humid environment for smaller C_D, similar to the cases with larger f. The potential intensity computed from this vertical profile shows a stronger sensitivity to C_D compared to the model results, especially for potential pressure intensity. Modifying the ambient rotation rate does not change this result.

We note that the recent modification to PI theory by Emanuel and Rotunno (2011) weakens the sensitivity to C_D.

The mean radius-height structure of the strongest TC within the domain for two SSTs is shown in Fig. 7. The boundary layer inflow and upper-tropospheric outflow characteristic of tropical cyclones is apparent, with an ascent region just inside of the radius of maximum surface wind (R_{mw}). As shown in Fig. 8, R_{mw} increases with SST, decreases with C_D and increases with f for small f (but saturates and probably decreases as f is increased further). The strongest storms that form for a given parameter setting have the smallest R_{mw}s. R_{mw}s simulated in this 25-km model are substantially larger than those observed (Stern and Nolan 2011). However we feel that the systematic variation seen in this model is of interest for comparison with high resolution simulation. We return to these results in section 4 where we show that quantitatively different results are obtained in smaller domains containing only one storm.

HZ08 explored the sensitivity of the natural extent of TCs to SST and f in the turbulent multi-storm equilibrium. With a higher resolution and a larger domain size, we hope to have a better estimate of this sensitivity. As shown in Fig. 9, the average number of TCs, n, doubles or halves as SST is perturbed by 4 K from the reference SST (301 K) and increases nearly linearly with f. We estimate the natural extent of TCs (r_0) as

$$r_0 = \sqrt{\frac{A}{n}} \tag{1}$$

in which A is the domain area. Two simple theoretical scalings for the Rossby radius of deformation NH/f, and the other is a natural length scale from PI theory V_p/f, where V_p is the potential intensity (Emanuel 1988). However, as shown in Fig. 9, while both of these two scalings project the right trend, neither satisfactorily captures the sensitivity. Modifying some of the choices in the computation of potential intensity, or using actual model intensities for the V_p/f scalings does not affect this conclusion. We will return to this topic in section 4.

4. Varying domain size

The sensitivity of rotating radiative-convective equilibrium to domain size is investigated by varying the domain size from $(1.25\times10^3\ \mathrm{km})^2$ to $(1.25\times10^4\ \mathrm{km})^2$, with SST at 301 K and f at 10°N. The composites of surface wind for different domain sizes are shown in Fig. 10. When the domain is small, only one tropical cyclone develops. The tropical cyclone has some elasticity in the sense that it can expand to fill the domain until multiple storms finally appear. Particularly, the extent of the single TC in the $(7.5\times10^3\ \mathrm{km})^2$ domain is nearly 20% larger than the natural extent of TCs in the $(1.25\times10^4\ \mathrm{km})^2$ domain.

The behavior of TCs evolves through four regimes, as illustrated by the time series of minimum surface pressure in each simulation (Fig. 11). When the domain is very small, only a tropical depression, with its central surface pressure at about 980 hPa, develops within the domain. As the domain size increases, the depression evolves into an intermittent tropical cyclone with intensity varying widely over a cycle of approximately 50 days. Further increase of the domain size avoids this collapse to weak intensity and leads to a sustained storm. Eventually, if the domain size becomes sufficiently large, multiple storms coexist. (We have conducted preliminary simulations analogous to these with a higher resolution non-hydrostatic model and see similar regime behavior, although the necessary domain size for a sustained storm is somewhat smaller.)

To see how the natural extent of TCs in turbulent equilibrium is related to this regime behavior, we conduct two series of experiments with : 1) different f at 5°N, 10°N and 20°N with SST at 301 K, and 2) different SST at 301 K and 305 K with f at 10°N. The time-mean central surface pressure is summarized in Fig. 12a and 12b respectively. The intensity first increases with domain size and then levels off approximately at the beginning of the regime of a single sustained storm (marked with an O symbol). This regime shifts towards large domain size as SST increases or f decreases, the same as the natural extent of TCs in turbulent equilibrium. For different parameter settings, the natural extent of TCs in turbulent equilibrium (marked with a | symbol) always falls in this regime. The following simple picture is consistent with these results: If the number of TCs increases from its equilibrium value, the available space for a given TC must decreases into the intermittent storm regime. This TC become unstable, and is more likely to be eliminated by competition with surrounding storms when sufficiently weak. The number of TCs then returns to its equilibrium value. On the other hand, if the number of TCs decreases, the suppression effect of TCs on its surrounding area becomes weak as TCs expand. With fewer but larger TCs randomly moving around, there is more free space for TC genesis. These two effects favor new TC genesis and bring the number of TCs back to its equilibrium.

One explanation for this regime of a sustained storm is that the available space for TCs needs to be sufficiently large to provide enough angular momentum to support the inner vortex. In addition to the two scales mentioned in section 3, a third candidate for the natural extent of TCs then comes up by relating the angular momentum at the outer radius r_0 to that at R_{mw}. For a reduction factor α between these two, this relationship can be written as $V_p R_{mw} = \frac{\alpha}{2} f r_0^2$. Assuming this reduction factor α is nearly invariant when SST or f varies, we have $r_0 \sim \sqrt{R_{mw} \frac{V_p}{f}}$. This is essentially the same relationship between R_{mw} and r_0 as in Emanuel and Rotunno (2011). As shown in Fig. 9, this scaling nicely captures the variation of r_0 with both SST and f except at very low SSTs. As we mentioned previously, the equilibrium achieved at very low SSTs, with a large number of weak TCs, looks very different from those with higher SST. The above argument may only apply to the cases where mature storms dominate. This parameter fit is a good description of the model results. However this relationship between r_0 and R_{mw} does not in itself provide a theory for r_0 or R_{mw}.

The variation of R_{mw} with parameters (SST, f and C_D) in lattice equilibrium, with domain size at 5000 km, is shown in Fig. 13. R_{mw} increases with f and decreases with SST and C_D. This result is consistent with that of Schecter and Dunkerton (2009) in which a three-layer tropical cyclone model is used, but different from what we found in turbulent equilibrium, for SST in particular (Fig. 8). The parameter sensitivity of R_{mw} in lattice equilibrium reflects the parameter sensitivity of the ratio between R_{mw} and TC extent r_0, since in a fixed size small domain r_0 is fixed, while the parameter sensitivity of R_{mw} in turbulent equilibrium takes into account both the parameter sensitivity of this ratio and that of r_0. As we discussed in section 3, TC extent r_0 can vary significantly with parameters in turbulent equilibrium. In this interpretation, the increase of r_0 with SST dominates over the decrease of $\frac{R_{mw}}{r_0}$ and results in increasing R_{mw} with SST in turbulent equilibrium (Fig. 8a), while the decrease of r_0 with f may offset the increase of $\frac{R_{mw}}{r_0}$ and leads to saturation or even decrease of R_{mw} for large f in turbulent equilibrium (Fig. 8b).

5. Conclusion and Discussion

Idealized models can be used to help fill the gap between theory and comprehensive climate model efforts. In much recent work, the spherical geometry is held fixed while the column physics and/or surface boundary condition are largely simplified. Instead, we choose to retain the column physics and simplify the geometry and surface boundary conditions. By coupling the column physics to the hydrostatic dynamics in a doubly-periodic domain, we can obtain a homogeneous doubly periodic rotating radiative-convective framework.

This study is along the line of Held and Zhao (2008), with the column physics replaced by that of a meso-scale resolution global atmospheric model, HiRAM, which produces quite realistic TC climatology when run with realistic boundary condition. A large domain $(2\times10^4\ \text{km})^2$ is used to obtain turbulent multi-storm equilibria. The parameter sensitivity is then studied by varying sea surface temperature, ambient rotation rate f and surface drag coefficient C_D. The mean TC intensity increases with SST and decreases with f and C_D. The potential intensity (Bister and Emanuel 2002a) calculated from the thermodynamic environment captures the sensitivity to SST and f with reasonable accuracy but overestimates that to C_D, especially in terms of central surface pressure. Note that PI theory in itself doesn't depend on f so an understanding of the dependence of the intensity on f requires a theory for the sensitivity of the model's equilibrated thermodynamic profiles to f.

The natural extent of TCs, r_0, in turbulent equilibrium increases with SST and decreases with f. Although we have some difficulty in estimating r_0 by simple theoretical scalings, we find it related to a shift in the regime behavior of lattice equilibrium, from a unsteady to a relatively stable mature storm. Such regime behavior is not unique in our model with meso-scale resolution and hydrostatic dynamics; we have also observed it in preliminary simulations using a high resolution non-hydrostatic model.

In turbulent equilibrium, the radius of maximum surface wind (R_{mw}) increases with SST, increases with f for small f but saturates or probably decreases as f is increased further. However in lattice equilibrium, R_{mw} decreases with SST and keeps increasing with f. This is because TC extent r_0 is constrained by the domain size in lattice equilibrium while in turbulent equilibrium r_0 varies systematically with environmental parameters. It is the relationship between R_{mw} and r_0 that is robust to change in domain size. Because of the poor resolution of the R_{mw} in this model, the results on the parameter sensitivity of R_{mw} are necessarily tentative.

We believe that simulations of rotating radiative-convective equilibrium such as these, with the resolution and column physics of a global atmospheric model being used to study the response of TCs to climate change, can provide a needed middle ground between the global model and non-hydrostatic cloud-resolving simulations in an idealized geometry that will help in establishing the strengths and limitations of the global simulations. This preliminary descriptive study is meant to help encourage further work along these lines.

Acknowledgments.

The authors thank Ming Zhao and Shian-Jiann Lin for making HiRAM available. We also thank Bruce Wyman for his work in configuring the doubly periodic model. Wenyu Zhou is partly supported by Award NA08OAR4320752 from National Oceanic and Atmospheric Administration (NOAA) Cooperative Institute for Climate Science, and partly by DOE award DE-SC0005189.

REFERENCES

Beljaars, A. C. M., 1995: The parametrization of surface fluxes in large-scale models under free convection. *Quarterly Journal of the Royal Meteorological Society*, **121 (522)**, 255–270.

Bister, M. and K. A. Emanuel, 2002a: Low frequency variability of tropical cyclone potential intensity 1. interannual to interdecadal variability. *Journal of Geophysical Research: Atmospheres*, **107 (D24)**, ACL 26–1–ACL 26–15.

Bister, M. and K. A. Emanuel, 2002b: Low frequency variability of tropical cyclone potential intensity 2. climatology for 1982–1995. *Journal of Geophysical Research: Atmospheres*, **107 (D22)**, ACL 5–1–ACL 5–4.

Bretherton, C. S., J. R. McCaa, and H. Grenier, 2004: A new parameterization for shallow cumulus convection and its application to marine subtropical cloud-topped boundary layers. part i: Description and 1D results. *Monthly weather review*, **132 (4)**, 864–882.

Brown, B. R. and G. J. Hakim, 2013: Variability and predictability of a three-dimensional hurricane in statistical equilibrium. *Journal of the Atmospheric Sciences*, **70 (6)**, 1806–1820.

Chen, J.-H. and S.-J. Lin, 2012: Seasonal predictions of tropical cyclones using a 25-km resolution general circulation model. *Journal of Climate*, 120713071748007.

Emanuel, K. and R. Rotunno, 2011: Self-stratification of tropical cyclone outflow. part i: Implications for storm structure. *Journal of the Atmospheric Sciences*, **68 (10)**, 2236–2249, doi:10.1175/JAS-D-10-05024.1.

Emanuel, K. A., 1988: The maximum intensity of hurricanes. *J. Atmos. Sci*, **45 (1)**, 143–1.

GAMDT, 2004: The new GFDL global atmosphere and land model AM2–LM2: evaluation with prescribed SST simulations. *Journal of Climate*, **17 (24)**, 4641–4673.

Hakim, G. J., 2011: The mean state of axisymmetric hurricanes in statistical equilibrium. *Journal of the Atmospheric Sciences*, **68 (6)**, 1364–1376, doi:10.1175/2010JAS3644.1.

Hakim, G. J., 2013: The variability and predictability of axisymmetric hurricanes in statistical equilibrium. *Journal of the Atmospheric Sciences*, **70 (4)**, 993–1005.

Held, I. M. and M. Zhao, 2008: Horizontally homogeneous rotating radiative-convective equilibria at GCM resolution. *Journal of the Atmospheric Sciences*, **65 (6)**, 2003–2013.

Lock, A. P., A. R. Brown, M. R. Bush, G. M. Martin, and R. N. B. Smith, 2000: A new boundary layer mixing scheme. part i: Scheme description and single-column model tests. *Monthly weather review*, **128 (9)**, 3187–3199.

Moorthi, S. and M. Suarez, 1992: Relaxed arakawa-schubert- a parameterization of moist convection for general circulation models. *Monthly Weather Review*, **120 (6)**, 978–1002.

Nolan, D. S. and E. D. Rappin, 2008: Increased sensitivity of tropical cyclogenesis to wind shear in higher SST environments. *Geophysical Research Letters*, **35 (14)**, n/a–n/a, doi: 10.1029/2008GL034147.

Nolan, D. S., E. D. Rappin, and K. A. Emanuel, 2007: Tropical cyclogenesis sensitivity to environmental parameters in radiative–convective equilibrium. *Quarterly Journal of the Royal Meteorological Society*, **133 (629)**, 2085–2107.

Schecter, D. A., 2011: Evaluation of a reduced model for investigating hurricane formation from turbulence. *Quarterly Journal of the Royal Meteorological Society*, **137 (654)**, 155–178.

Schecter, D. A. and T. J. Dunkerton, 2009: Hurricane formation in diabatic ekman turbulence. *Quarterly Journal of the Royal Meteorological Society*, **135 (641)**, 823–838.

Stern, D. P. and D. S. Nolan, 2011: On the vertical decay rate of the maximum tangential winds in tropical cyclones. *Journal of the Atmospheric Sciences*, **68 (9)**, 2073–2094.

Zhao, M. and I. M. Held, 2010: An analysis of the effect of global warming on the intensity of atlantic hurricanes using a GCM with statistical refinement. *Journal of Climate*, **23 (23)**, 6382–6393.

Zhao, M., I. M. Held, and S.-J. Lin, 2012: Some counterintuitive dependencies of tropical cyclone frequency on parameters in a GCM. *Journal of the Atmospheric Sciences*, **69 (7)**, 2272–2283.

Zhao, M., I. M. Held, S. J. Lin, and G. A. Vecchi, 2009: Simulations of global hurricane climatology, interannual variability, and response to global warming using a 50-km resolution GCM. *Journal of Climate*, **22 (24)**, 6653–6678.

List of Figures

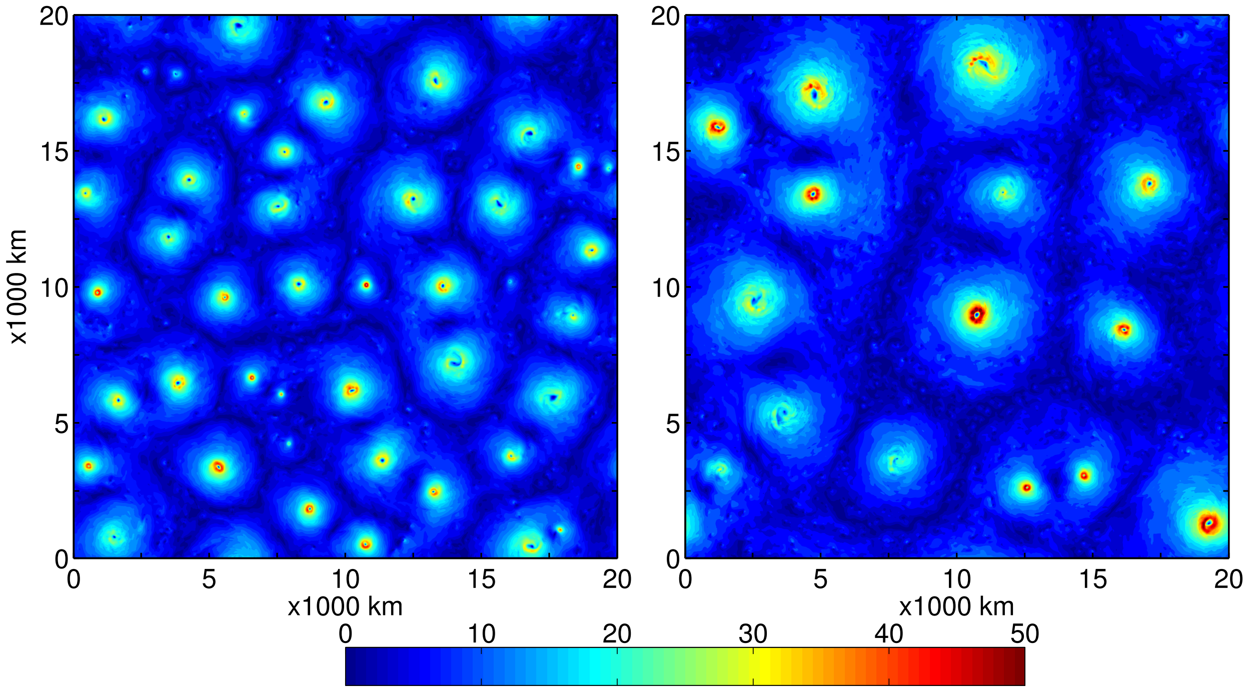

Fig. 1. Snapshots of surface wind (m s^{-1}) for different sea surface temperatures. (left) SST= 297 K; (right) SST = 305 K. Ambient rotation rate f is set at 20°N.

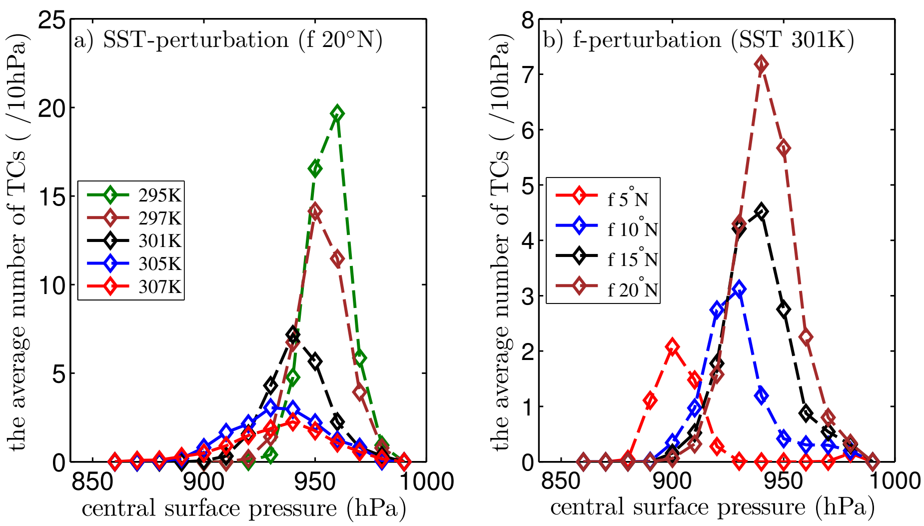

FIG. 2. (a) The average number of TCs in the domain with their central surface pressures within the specified 10 hPa interval, as a function of SST. Ambient rotation rate f is set at 20°N. (b) As in (a), but for the sensitivity to ambient rotation rate f . SST is fixed at 301 K. For both sets of experiments, surface exchange coefficients are calculated from Monin-Obukhov scheme.

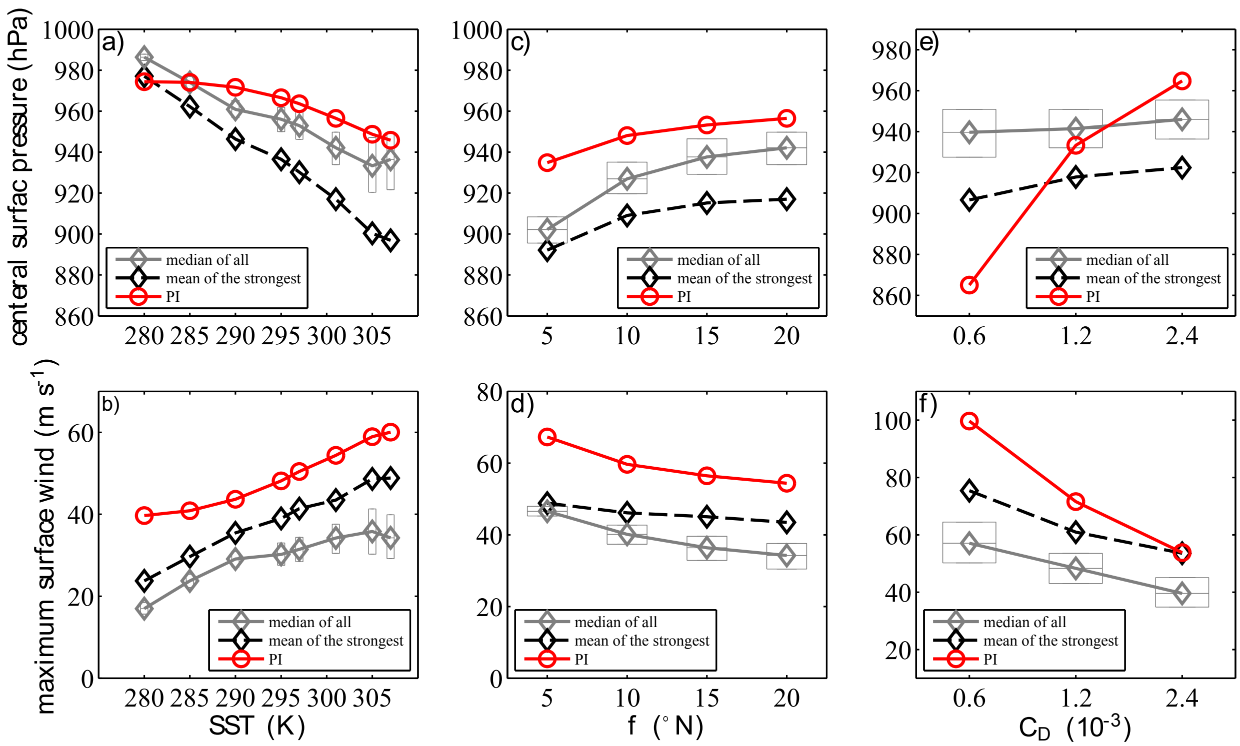

FIG. 3. (a) The gray line is the median central surface pressure as a function of SST of all collected TCs. The 25th and 75th percentiles coincide with the edges of the gray box. The black line shows the mean of the strongest storms at each instant of time. The red line shows the estimate from potential intensity theory using the domain- and time-mean thermodynamical profile. (b) As in (a), but for maximum surface wind. SST varies from 280 K to 307 K. Ambient rotation rate f is fixed at 20°N. (c), (d) are similar to (a) and (b), but for the sensitivity to ambient rotation rate f . SST is fixed at 301 K. For both sets of experiments, surface exchange coefficients are calculated from Monin-Obukhov scheme. (e), (f) show the sensitivity to surface drag coefficient C_D. Surface drag coefficient C_D varies from 0.6×10^{-3} to 2.4×10^{-3} with surface exchange coefficient for enthalpy C_k fixed at 1.2×10^{-3}. Ambient rotation rate f is fixed at 15°N and SST is 301 K.

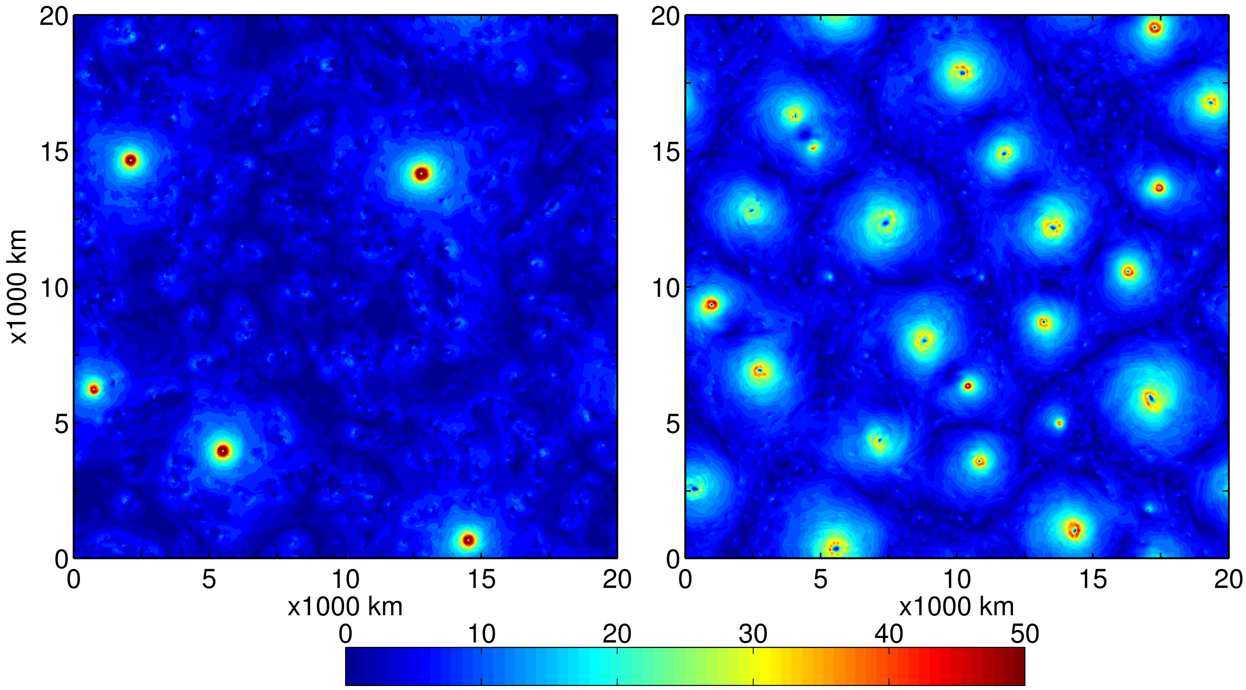

FIG. 4. Snapshots of surface wind (m s^{-1}) for different ambient rotation rates. (left) f at 5°N; (right) f at 20°N. SST is fixed at 301 K.

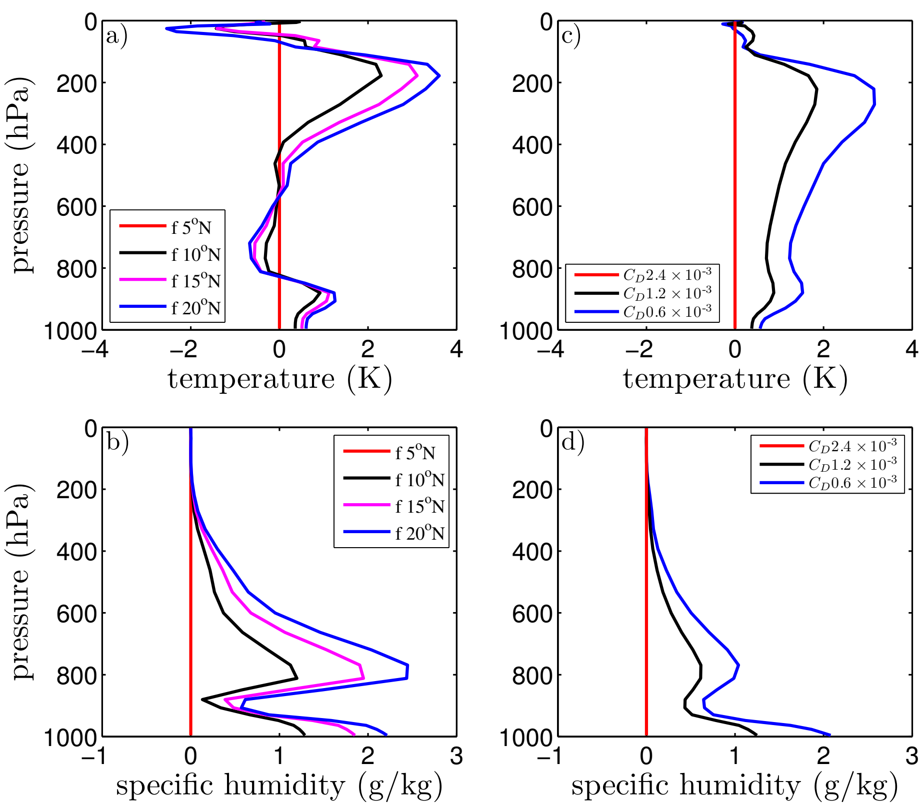

Fig. 5. (a, b) Differences in vertical profiles of temperature and specific humidity between different ambient rotation rates (vs 5°N case) with surface exchange coefficients calculated from Monin-Obukhov scheme. and (c, d) surface drag coefficients (vs $C_D = 2.4\text{x}10^{-3}$ case) with ambient rotation rate at 15°N. SST is fixed at 301 K.

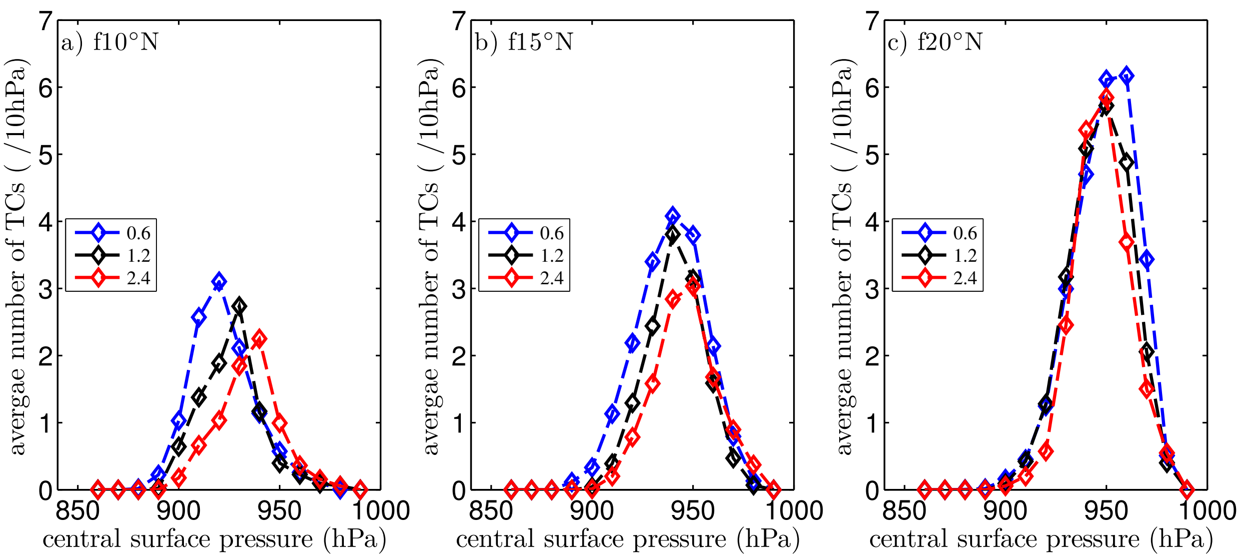

FIG. 6. (a) The average number of TCs in the domain with their central surface pressures within the specified 10 hPa interval as a function of surface drag coefficient C_D (0.6, 1.2, 2.4 $\times 10^{-3}$) with ambient rotation rate f set at 10°N. (b) (c) As in (a), but with ambient rotation rate f set at 15°N and 20°N. Surface exchange coefficient for enthalpy C_k is fixed at 1.2×10^{-3} and SST is 301 K.

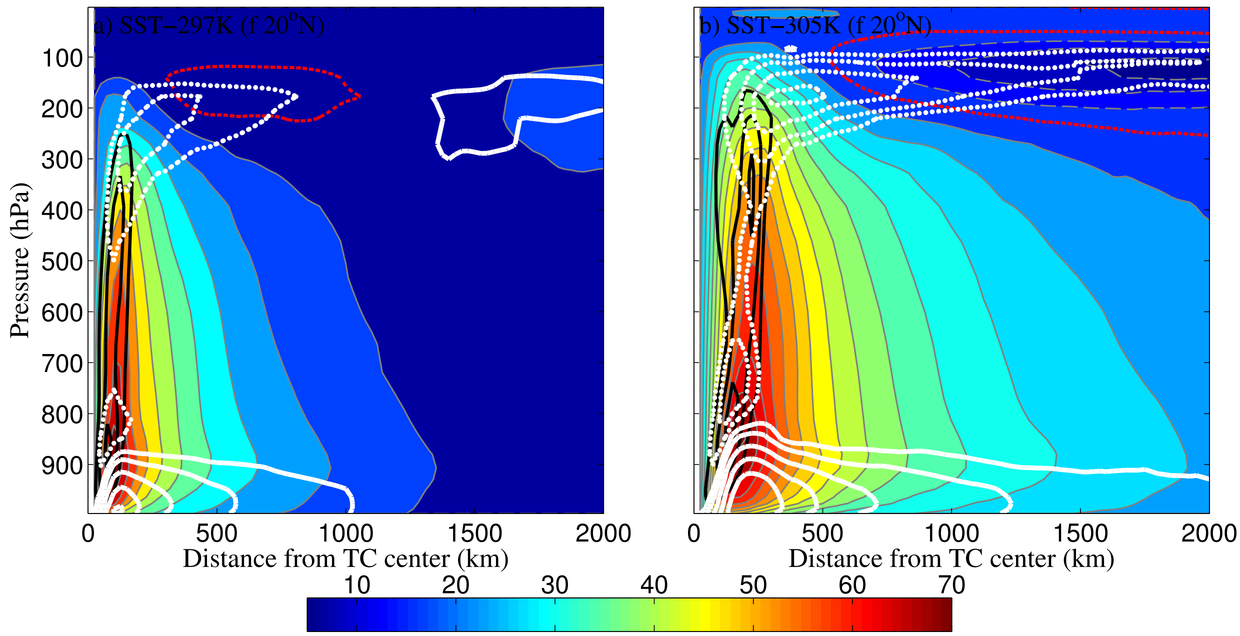

Fig. 7. Time-mean and azimuthal-mean tangential (colors), radial (white) and vertical (black) velocities of the strongest tropical cyclone for sea surface temperature a) 297 K and b) 305 K. Tangential winds are contoured every 5 m s^{-1}. Positive (cyclone) values are solid, negative (anticyclone) values are dashed, and the zero contour is a red dashed line. Radial winds are contoured at [2,5,10,15,20] m s^{-1}. Positive (outflow) values are dashed, negative (inflow) values are solid, and the zero contour is omitted. Vertical velocity is contoured (negative only) at -1, -2, and -3 Pa s^{-1}. Ambient rotation rate f is fixed at 20°N.

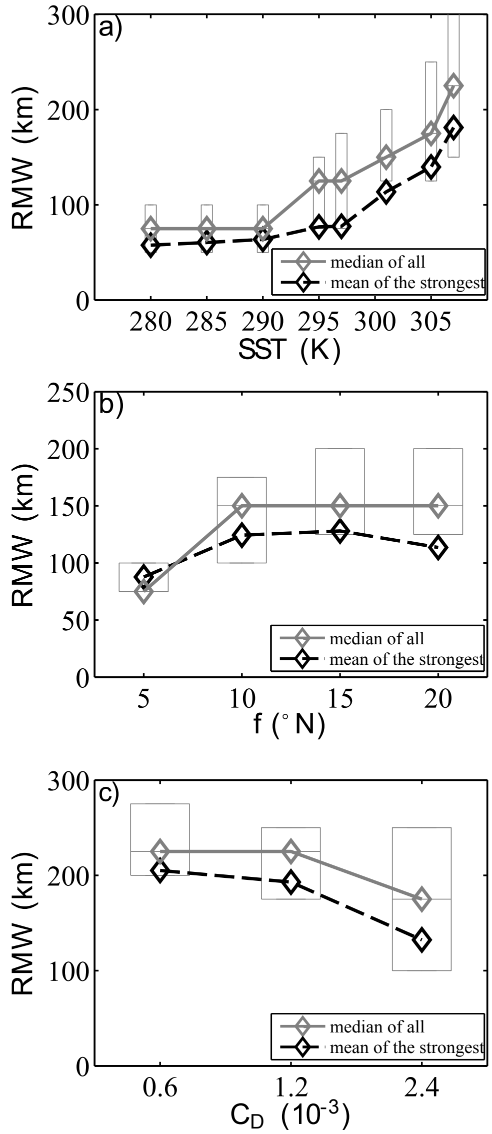

FIG. 8. (a) The gray line is the median R_{mw} of all collected TC as a function of SST. The 25th and 75th percentiles coincide with the edges of the gray box. The black line shows the mean R_{mw} of the strongest storms at each instant of time. SST varies from 280 K to 307 K. Ambient rotation rate f is fixed at 20°N. (b) as in (a), but for the sensitivity to ambient rotation rate f . SST is fixed at 301 K. For both sets of experiments, surface exchange coefficients are calculated from Monin-Obukhov scheme. (c) are those for the sensitivity to surface drag coefficient C_D. Surface drag coefficient C_D varies from 0.6×10^{-3} to 2.4×10^{-3} with surface exchange coefficient for enthalpy C_k fixed at 1.2×10^{-3}. Ambient rotation rate f is fixed at 15°N and SST is 301 K.

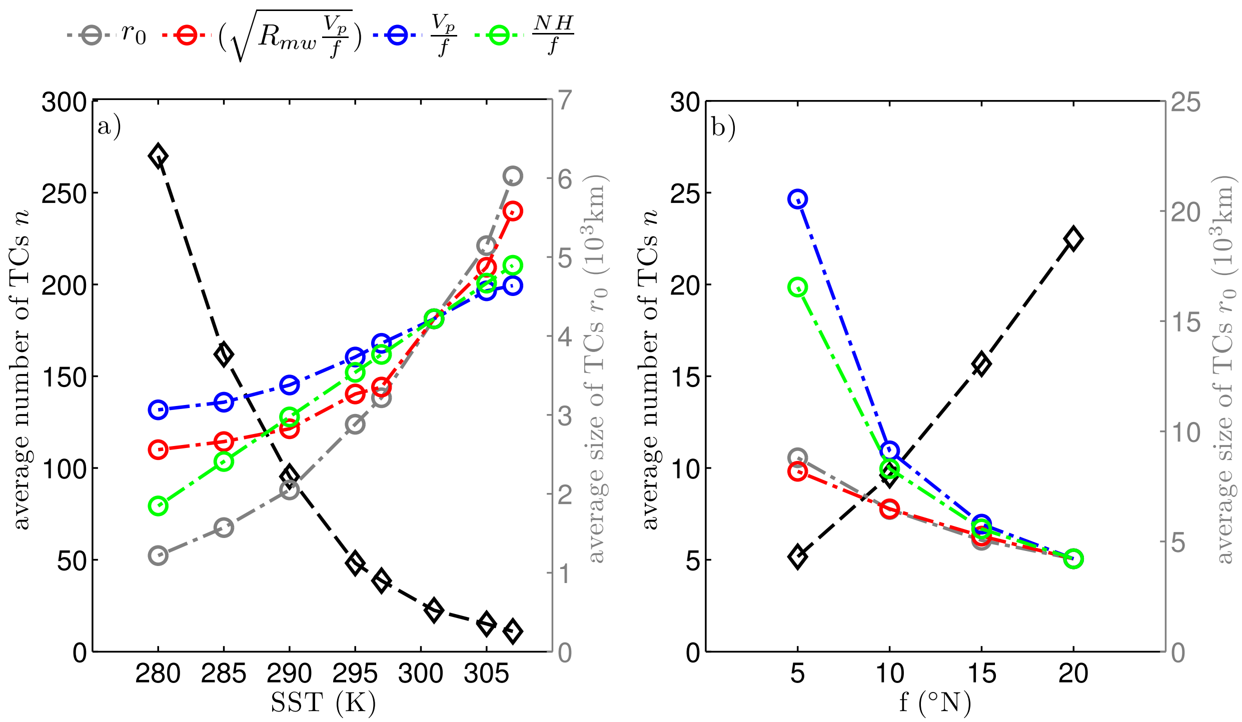

FIG. 9. (a) The average number of TCs n (black-dash line with diamond) and the natural extent of TCs r_0 ($\sqrt{\frac{A}{n}}$, gray dash-dot line with circle) as a function of SST. Ambient rotation rate f is set at 20°N. Three possible scalings are shown. Red line: $\sqrt{R_{mw}\frac{V_p}{f}}$, discussed in section 4; blue line: $\frac{V_p}{f}$; green line: $\frac{NH}{f}$. (b) As in (a) but for the variation of ambient rotation rate f. The underlying SST is 301 K. The estimates from these three scalings are normalized to the natural extent of TCs with SST at 301 K and f at 20°N.

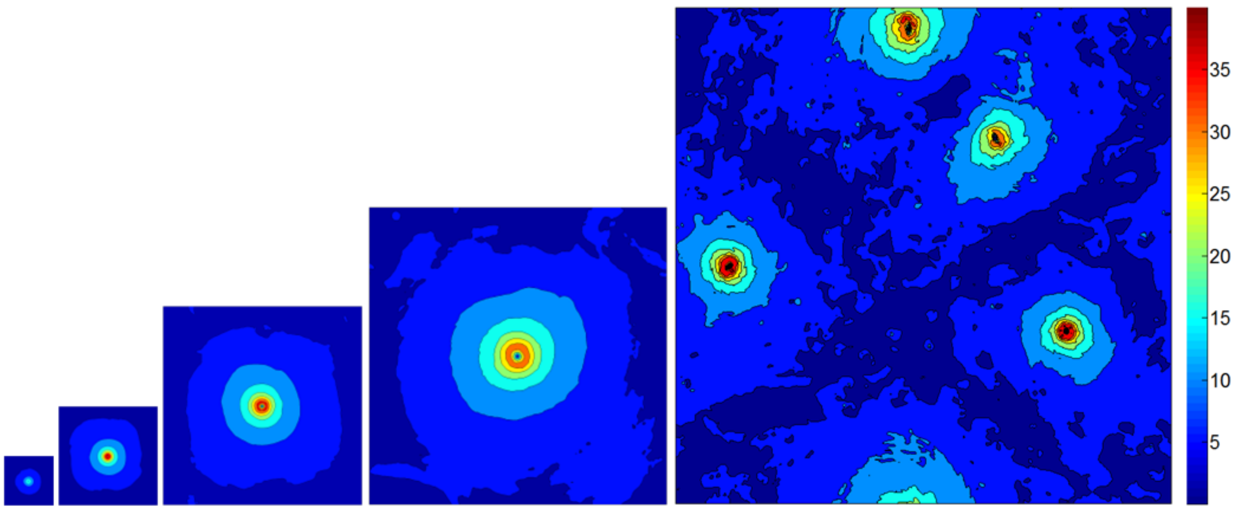

FIG. 10. Composite of surface wind for simulations with domain sizes at 1250 km, 2500 km, 5000 km, 7500 km and snapshot of surface wind for domain size at 12500 km, all with SST at 301 K and f at 10°N.

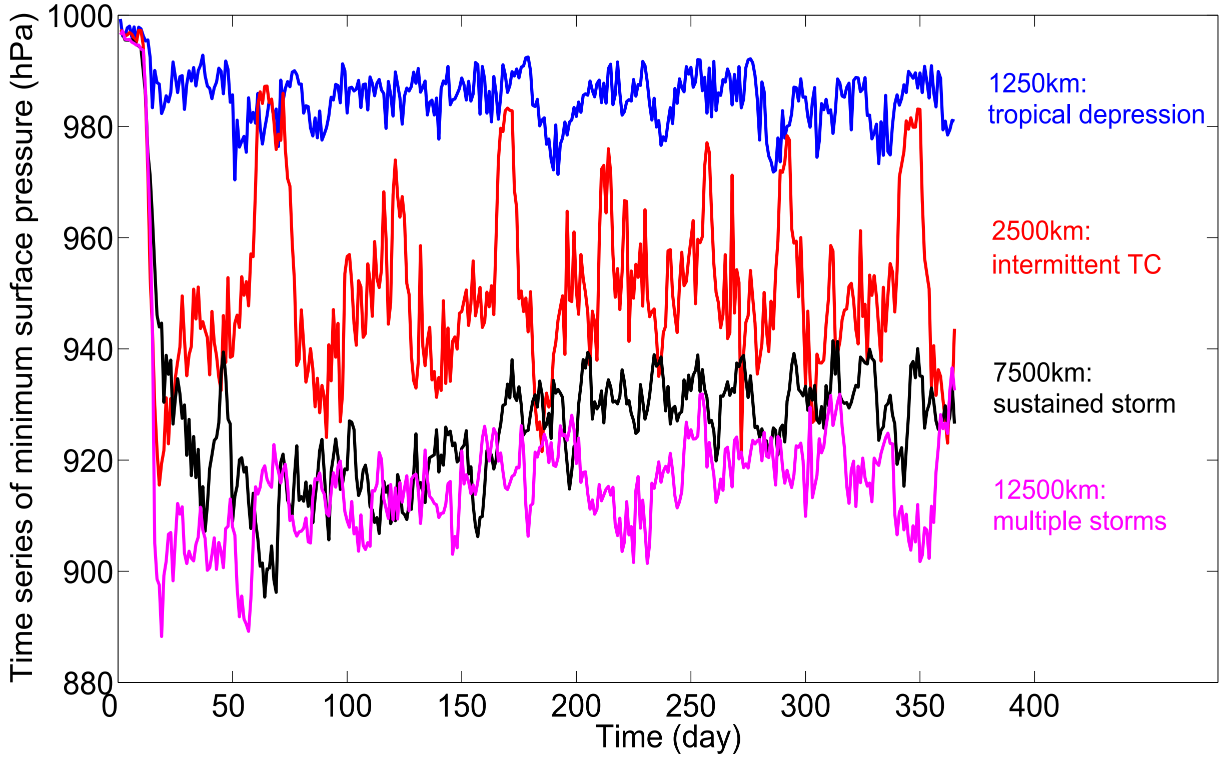

FIG. 11. Time series of minimum surface pressure for different regimes. SST is 301 K and ambient rotation rate f is fixed at 10°N.

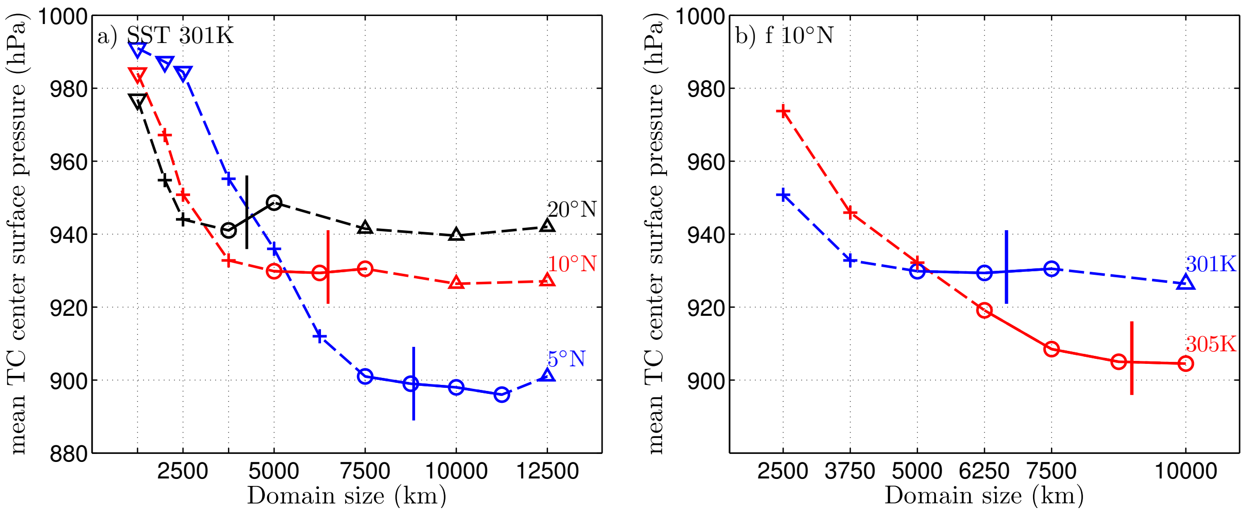

FIG. 12. Time mean TC central surface pressure as a function of domain sizes at (a) different ambient rotation rates and (b) sea surface temperatures. The four regimes mentioned above are marked with different symbols, ∇ (tropical depression), $+$ (intermittent storm), $\circ$ (sustained storm) and $\triangle$ (multiple storms). The average scale of TCs in corresponding large domain simulation is marked with a $|$ symbol.

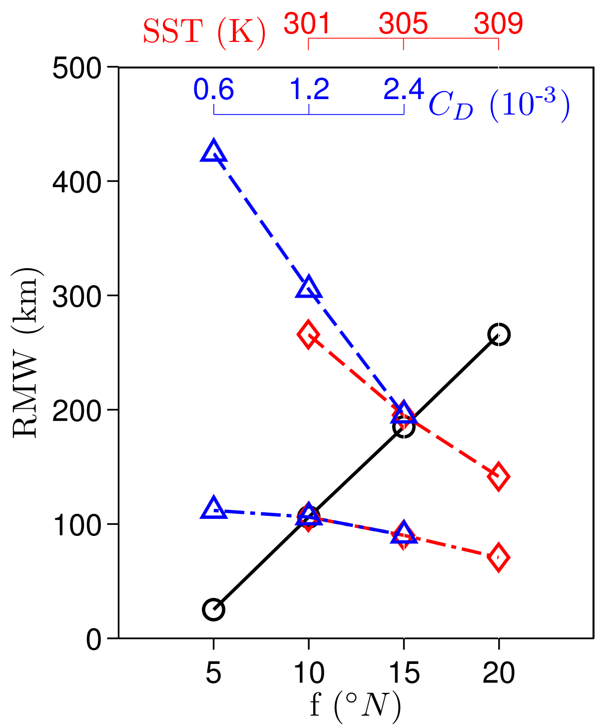

FIG. 13. Sensitivity of R_{mw} to f (black line), SST (red line) and C_D (blue line) in a fix size small domain (5000 km on a side). In f and C_D perturbation experiments, SST is fixed at 301 K. For both SST and C_D perturbation, two series of experiments with ambient rotation rates set at 10°N (dash-dot line) and 20°N (dash line) are conducted.